

Ruthenocuprates $\text{RuSr}_2(\text{Eu,Ce})_2\text{Cu}_2\text{O}_{10-y}$: Intrinsic magnetic multilayers

I.Živković,¹ Y.Hirai,² B.H.Frazer,² M.Prester,^{1,*} D.Drobac,¹ D.Ariosa,³
H.Berger,³ D.Pavuna,³ G.Margaritondo,³ I.Felner,⁴ and M.Onellion^{2,†}

¹*Institute of Physics, P.O.B.304, HR-10 000, Zagreb, Croatia*

²*Physics Department, University of Wisconsin, Madison, WI 53706, U.S.A.*

³*Institut de Physique Appliquée, École Polytechnique Fédérale de Lausanne, CH-1012 Lausanne, Switzerland*

⁴*Racah Institute of Physics, Hebrew University, Jerusalem, Israel*

(Dated: October 30, 2018)

We report ac susceptibility data on $\text{RuSr}_2(\text{Eu,Ce})_2\text{Cu}_2\text{O}_{10-y}$ (Ru-1222, Ce content $x=0.5$ and 1.0), $\text{RuSr}_2\text{GdCu}_2\text{O}_8$ (Ru-1212) and SrRuO_3 . Both Ru-1222 ($x=0.5, 1.0$) sample types exhibit unexpected magnetic dynamics in low magnetic fields: logarithmic time relaxation, switching behavior, and ‘inverted’ hysteresis loops. Neither Ru-1212 nor SrRuO_3 exhibit such magnetic dynamics. The results are interpreted as evidence of the complex magnetic order in Ru-1222. We propose a specific multilayer model to explain the data, and note that superconductivity in the ruthenocuprate is compatible with both the presence and absence of the magnetic dynamics.

PACS numbers: 74.27.Jt, 74.25.Ha, 75.60.Lr, 75.70.Cn

I. INTRODUCTION

Coexistence of superconductivity and long-range magnetic order, and the types of magnetic order compatible with superconductivity, are problems of widespread interest¹. Such systems include the ruthenocuprates, which exhibit superconductivity in the CuO_2 planes² with some type(s) of long-range magnetic order that involves at least the RuO_2 planes^{3,4}. One of the main issues for the ruthenocuprates is the nature of long-range magnetic order coexisting with superconductivity. The issue is complicated because, as previous work (muon spin rotation⁴, magnetic resonance⁵, and neutron diffraction⁶) has shown, there is evidence- even in the simple Ru-1212 material- for both ferromagnetic^{4,5} and antiferromagnetic⁶ ordering. Both magnetization⁷ and NMR² studies of Ru-1212 materials confirm the presence of a ferromagnetic component of the low temperature magnetic order. Theoretical calculations⁸ of the electronic structure predict antiferromagnetic order for Ru-1212.

There is an implicit assumption that all ruthenocuprates will possess the same long-range magnetic order. As we show below, this is not the case for the data we measured, comparing Ru-1212 and Ru-1222, nor is it the case for the existing literature. Neutron diffraction measurements have not been reported for Ru-1222. Magnetization, low frequency susceptibility, and Mössbauer/NQR reports^{3,9} indicate a pronounced- perhaps even a dominant- role of ferromagnetism in the spontaneous magnetic order of Ru-1222. The main result of our report is that Ru-1222 samples exhibit unexpected dynamical magnetic features in very low magnetic fields. We have measured the AC susceptibility while varying the dc magnetic field either continuously or in steps. We found a pronounced susceptibility ‘switching’, logarithmic time relaxation, and hysteretic, inverted-in-sense, susceptibility butterfly loops. While these properties have been individually reported earlier in other, non-superconducting magnetic

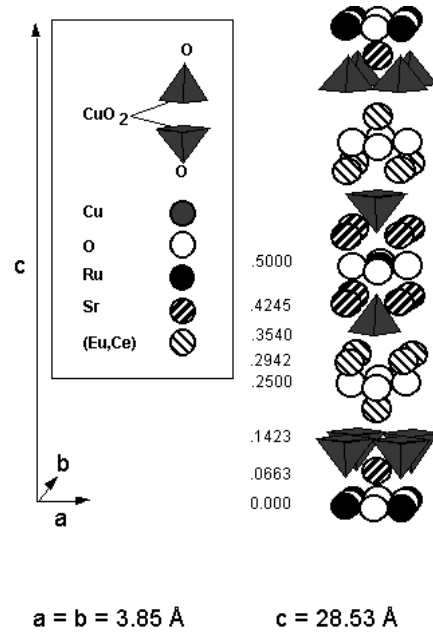


FIG. 1: Unit cell of Ru-1222 ruthenocuprate

systems, the Ru-1222 system exhibits all of these properties. The inverted butterfly hysteresis represents, to our knowledge, the first observation of this phenomenon in a bulk magnetic system. The contrast between Ru-1222 and Ru-1212 (or SrRuO_3) samples is marked: neither Ru-1212 nor SrRuO_3 exhibit any of these dynamical magnetic properties. Following the data, we present a model in which we argue that the magnetic ordering of Ru-1222 involves both ferromagnetic and antiferromagnetic coupling, and that Ru-1222 is a rare example of an intrinsic, naturally grown magnetic multilayer system with the layers coupled with antiferromagnetic interactions, similar to that inferred of the $(\text{La,Sr})_3\text{Mn}_2\text{O}_7$ colossal magnetoresistance manganite¹⁰.

II. EXPERIMENTAL

Polycrystalline samples of Ru-1222, Ru-1212 and SrRuO_3 were fabricated as published elsewhere^{3,11}. Two Eu/Ce stoichiometries of Ru-1222 were synthesized: 'superconducting' (Ce content $x=0.5$) and 'insulating' (Ce content $x=1.0$). SrRuO_3 served as a three dimensional, ferromagnetic reference material. In all three materials, magnetic order stems from the RuO_6 octahedra. We used x-ray diffraction (data not shown) to establish that all samples were crystallographically single phase. We measured the sample microstructure using scanning electron microscopy (SEM), with results shown in Figure 2. AC susceptibility data were taken using a CryoBIND system¹² calibrated for absolute susceptibility results. The AC susceptibility measurements used a frequency of 230 Hz, an ac magnetic field of 0.15 Oe, and a dc magnetic field between 0-100 Oe. DC susceptibility measurements of some samples were obtained using a Lake Shore vibrating-sample magnetometer (VSM).

III. RESULTS

Figure 1 illustrates the Ru-1222 unit cell. Notice the large separation along the c-axis between RuO_2 planes; we return to this point below. Figure 2 illustrates the microstructure. Ru-1222 ($x=1.0$) samples exhibit a dense structure with almost no isolated grains and very small intergranular regions; grain boundaries were difficult to identify. Ru-1222 ($x=0.5$) and Ru-1212 samples, by contrast, exhibit well-defined grains (size typically $1 - 2\mu\text{m}$) and pronounced grain boundaries. As we note further below, there are marked, qualitative differences between the Ru-1212 samples and Ru-1222 samples of either stoichiometry. Fig. 2 is thus important because it rules out grain structure as the source of these qualitative differences.

Figure 3 shows the AC susceptibility data of Ru-1212, Ru-1222 ($x=0.5$) and Ru-1222 ($x=1.0$). Ru-1212 exhibits a single maximum at $T_N=133$ K. By contrast, both Ru-1222 samples exhibit peaks at lower temperature T_M ($=85$ K ($x=0.5$) and 117 K ($x=1.0$)) and a broad feature between 120-140 K, followed by non-Curie-Weiss behavior extending up to 180K. We discuss possible interpretations of the broad features and non-Curie-Weiss behavior separately¹³.

In this work we primarily focus the magnetically ordered ($T < T_M$) phase of both ruthenocuprates and report hysteretic and highly nonlinear magnetic dynamics characterizing Ru-1222, but not Ru-1212, samples. Figures 4-10 illustrate different aspects of the AC susceptibility response of Ru-1222, pointing out the differences in the equivalent response of Ru-1212 under similar experimental conditions. Although we show only the results for $x=0.5$ or $x=1.0$ compositions of the Ru-1222 ruthenocuprate in a particular figure, both stoichiometries exhibit the same qualitative behavior in all respects.

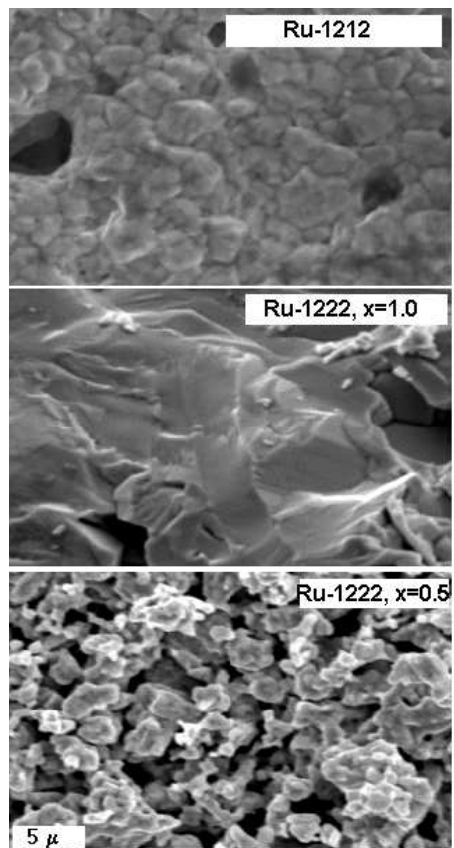


FIG. 2: Scanning electron microscopy images of Ru-1212 (top panel), Ru-1222, $x=1.0$ (middle panel), and Ru-1222, $x=0.5$ (bottom panel)

We first report on AC susceptibility temperature dependence in small (< 100 Oe) applied dc magnetic fields. Figs. 4, 5 illustrates a sequence of temperature dependences of zero-field cooled (ZFC) AC susceptibility measurement in several dc magnetic fields at temperatures near the peak value for Ru-1222 ($x=0.5$ and $x=1.0$) sam-

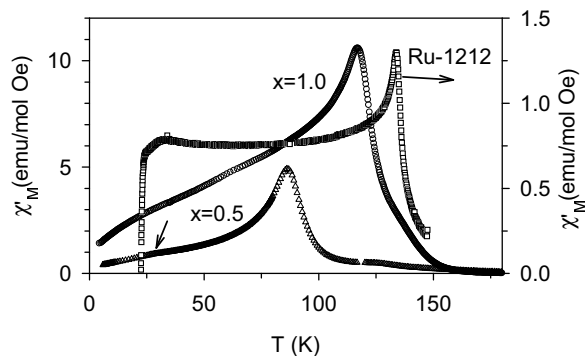


FIG. 3: Ac susceptibility measurements of Ru-1222 ($x=0.5$ and $x=1.0$) and Ru-1212 samples. Note different scales for the two sample types. Vertical arrow indicates the kink attributed to superconductivity in Ru-1222, $x=0.5$, sample.

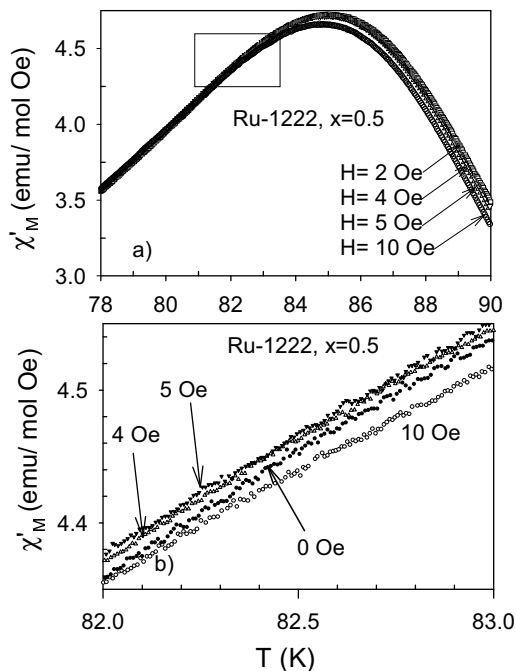


FIG. 4: Temperature dependence of ZFC ac susceptibility of Ru-1222, $x=0.5$, sample in a sequence of small applied magnetic fields. The panel a) would suggest collapsing of all of the curves below the ordering maximum inside the 10 Oe magnetic field range. A closer inspection of the rectangular area, shown in b) on expanded scale, indicates that below the ordering maxima there is actually a non-monotonic change of ac susceptibility as the applied magnetic field increases.

ples. These figures show that there is a range of dc magnetic field values, and temperatures, for which the AC susceptibility of Ru-1222 samples increases as the dc magnetic field increases. By contrast, Ru-1212 and SrRuO₃ samples exhibit ‘normal’ behavior: at all temperatures, the AC susceptibility monotonically decreases for increasing dc magnetic fields. Qualitatively, ‘normal’ behavior is easy to interpret: AC susceptibility measures how free the magnetic moments are to perform forced oscillations imposed by the ac magnetic field. Therefore, any superimposed dc magnetic field introduces a further restriction on the oscillations, and the AC susceptibility decreases. Fig. 5 illustrates AC susceptibility for Ru-1222 ($x=1.0$) samples. Note the common qualitative trend shown in Fig. 4: below T_M the AC susceptibility versus dc magnetic field exhibits non-monotonic behavior with increasing dc magnetic field, while for temperatures above T_M the AC susceptibility decreases monotonically with increasing dc magnetic field. The unexpected increase in AC susceptibility from zero dc field to the ‘turning field’ (= the dc field at which the AC susceptibility is a maximum) reaches as much as 15% for Ru-1222 ($x=1.0$). It is much less ($\approx 0.5\%$) for Ru-1222 ($x=0.5$), and the magnitude of the turning field is lower for Ru-1222 ($x=0.5$) than for Ru-1222 ($x=1.0$). For some samples we also noted small, quasi-periodic jumps in the tem-

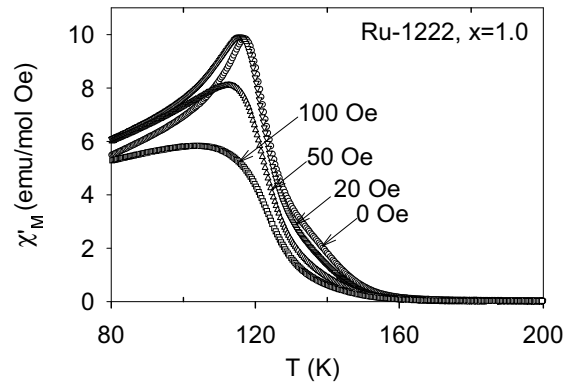


FIG. 5: Temperature dependence of ZFC ac susceptibility of Ru-1222, $x=1.0$, sample versus applied dc magnetic field. Below the ordering maxima, the susceptibility exhibits non-monotonic behavior versus applied magnetic field.

perature dependence of the AC susceptibility below T_M , similar to the jumps recently reported for certain manganese samples¹⁴. Because the occurrence of these oscillations/jumps were not reproducible in repeated measurements, we did not perform any systematic studies of this effect on our samples.

A. Time dependence of AC susceptibility

We measured the time response of the AC susceptibility to different dc magnetic fields at several fixed temperatures. We would zero-field cool the sample to a fixed temperature, apply a dc field and take the measurement of time dependence, then- in zero dc magnetic field- raise the temperature to above 180K and lower the temperature (to the same or another fixed temperature) before repeating the measurement with different dc field. Fig. 6 illustrates some of the results. The inset of Fig. 6a shows how the dc magnetic field was abruptly turned on and off. Figs. 6a) and b) shows that the AC susceptibility sharply increaseses (‘switches’) when the dc magnetic field is turned on. After the AC susceptibility switch, there is a gradual decrease. In Figs. 6a) and b), note that even after 2000 sec. the AC susceptibility has not returned to the initial value. The AC susceptibility exhibits a strong time relaxation. Such relaxation -often called disaccommodation^{15,16}- has been reported previously for other magnetic systems¹⁵. The data in Figs. 6a) and b) are, however, surprising in certain respects: the AC susceptibility *increases* above the ZFC value when a dc magnetic field is applied. As Fig. 6c shows, the AC susceptibility relaxes slowly, and logarithmically, and does not return to the ZFC value on the time scale of at least one day (the longest period we measured at one dc field and temperature). The data indicate:

- a) A step-like change of the dc magnetic field causes i) the AC susceptibility to switch to a new value, and ii) the

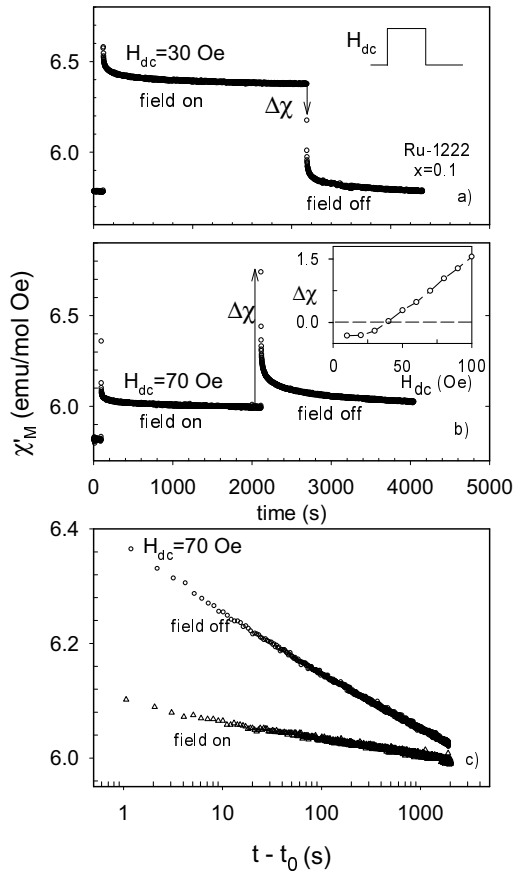


FIG. 6: a) Ac susceptibility versus time for Ru-1222, $x=1.0$ at 80K, with $H_{dc} = 0\text{Oe}$ initially, then $H_{dc} = 30\text{Oe}$, and finally $H_{dc} = 0\text{Oe}$, shown schematically in the Inset. ($\Delta\chi$), defined as change in susceptibility immediately after H_{dc} is switched off, is negative. Note relaxation of susceptibility. b) All conditions the same as in a) except $H_{dc} = 70\text{Oe}$. ($\Delta\chi$) is positive for this value of H_{dc} . Note relaxation of susceptibility. Inset: Overshoot $\Delta\chi$ (in units of emu/moleOe) at 80K versus H_{dc} . Note change from negative (no overshoot) to positive (overshoot) at $H_{dc} \approx H_{sf}$. c) Ac susceptibility versus logarithm of time for Ru-1222, $x=1.0$, with $H_{dc} = 70\text{Oe}$ and 80K. (t_0) is time at which H_{dc} is either switched on or off. Data for both *field on* and *field off* conditions are included.

ZFC equilibrium state changes to a metastable magnetic state. The magnitude of the AC susceptibility change ($\Delta\chi$) (Fig. 6a,b) is positive when H_{dc} is turned on, and can be either positive or negative when H_{dc} is turned off. The metastable magnetic state exhibits logarithmic relaxation, a phenomenon variously ascribed to disaccommodation^{15,16} or magnetic aftereffect¹⁷. It is particularly noteworthy, as Fig. 7 illustrates, that Ru-1212 samples do not exhibit any indication of AC susceptibility relaxation;

b) The AC susceptibility relaxation is logarithmic in time for both H_{dc} on and H_{dc} off, and follows the functional form $\chi(t) = \chi_0[1 - \alpha \ln(t - t_0)]$. The parameters χ_0 and the relaxation rate α depend on temperature, H_{dc} ,

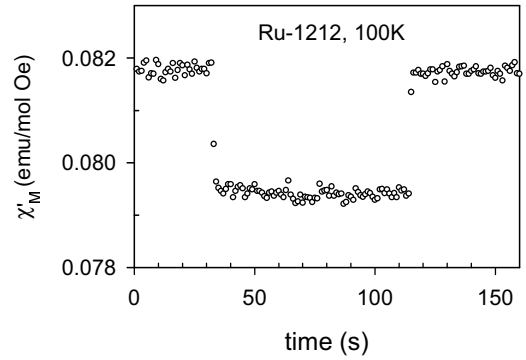


FIG. 7: Ac susceptibility versus time for Ru-1212 at 100K in the applied rectangular pulse of magnetic field, as specified in Fig.6a. No time relaxations can be detected in Ru-1212 sample.

and the magnetic history (whether H_{dc} was turned on or off);

c) For $|H_{dc}|$ above a threshold value of 40 Oe, when H_{dc} is turned off there is a pronounced ‘overshoot’ phenomenon with a sizeable positive ($\Delta\chi$) (see Fig. 6b);

d) Surprisingly, applying a rectangular field pulse results in a magnetic state with an *increased* AC susceptibility (Fig. 6). The logarithmic relaxation over several decades of time indicates that the excited AC susceptibility persists.

B. AC susceptibility in sweeping magnetic field: Observation of inverted hysteresis

We also swept the dc magnetic field in an almost continuous fashion, with increments typically of 1 Oe. The most striking behavior, as shown in Fig. 8, is observing an inverted hysteresis phenomenon for Ru-1222 that is also entirely absent for Ru-1212 or SrRuO₃. To measure the classic magnetization hysteresis, one ramps the applied magnetic field (H) from positive to negative and back, and continuously measures the magnetization $M(H)$. In a similar, ‘butterfly’ hysteresis technique¹⁸, the AC susceptibility $\chi_{ac}(H)$, is measured rather than the magnetization. Generally, these two hysteresis loops yield similar information¹⁹. For instance, the characteristic maxima in butterfly hysteresis (Figs. 8, 9) define the coercive field¹⁸. Fig. 8a shows typical butterfly hysteresis data taken for Ru-1222 and Ru-1212 samples. The data establish that the two types of ruthenocuprates exhibit qualitatively different responses. There are also pronounced differences between the Ru-1222 data and the results for SrRuO₃ (Fig. 9a). The most striking difference is the inverted sense of loop circulation for Ru-1222: the AC susceptibility signal is consistently larger for the field-decreasing branch compared to the field-increasing branch. To our knowledge, this is the first observation of inverted butterfly loops in a bulk magnetic system. The numerical integration of the butterfly hysteresis is shown

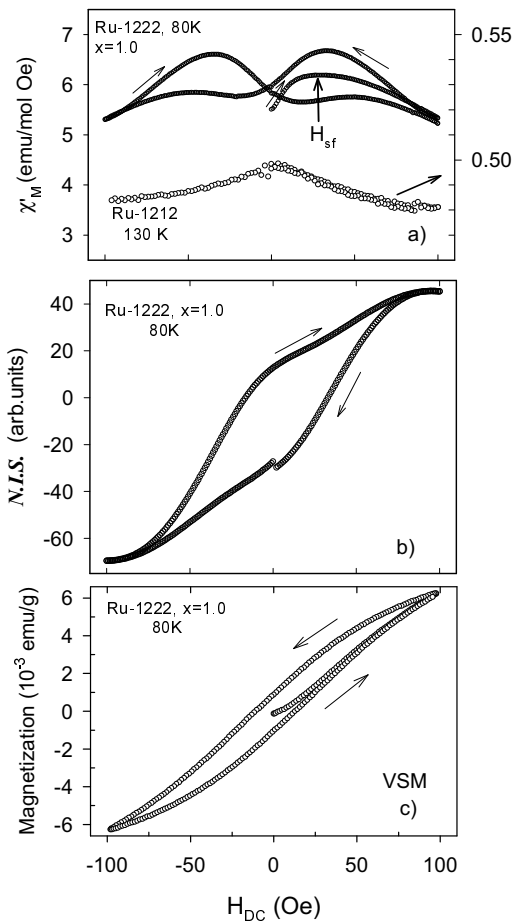


FIG. 8: a) Left axis: ‘Butterfly’ hysteresis for Ru-1222, $x=1.0$ at 80K. Right axis: Analogous data for Ru-1212, just below magnetic ordering temperature. Unlike Ru-1222, note for Ru-1212 a monotonic decrease in ac susceptibility with increasing magnitude of the dc magnetic field, and no hysteresis. b) Numerical integral $NIS \equiv \int_0^H \chi(h)dh$ of butterfly susceptibility shown in a) versus H_{dc} for Ru-1222. The units are arbitrary. Note the inverse hysteresis loop. c) DC (vibrating-sample) magnetization hysteresis for the same Ru-1222 sample as in a). A normal (counter-clockwise) circulations is observed.

for Ru-1222 (Fig. 8b) and SrRuO₃ (Fig. 9b). While the results for SrRuO₃ exhibit the counter-clockwise pattern of the usual magnetization hysteresis, the integrated butterfly of the Ru-1222 sample exhibits an inverted (clockwise) hysteresis loop. It is noteworthy that the vibrating-sample magnetometer measurements on the same Ru-1222 (Fig. 8c) shows the dc magnetization hysteresis loop with a ‘normal’ (counter-clockwise) sense of circulation. Therefore, the inverted hysteresis phenomenon represents a unique, dynamical feature of the Ru-1222 system, arising from the field-induced and AC magnetic field-assisted metastable magnetic states observed in Fig. 6. Other noteworthy features of the Ru-122 butterfly hysteresis include: i) the presence of a maximum even in the ZFC (virgin) curve, ii) pronounced dependence on the observ-

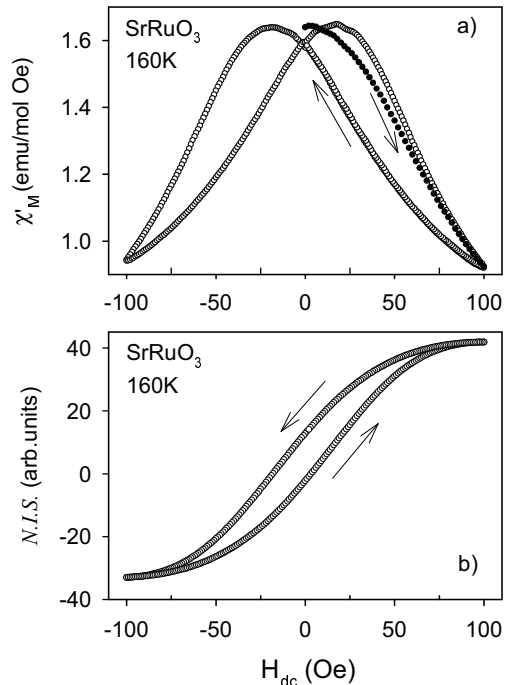


FIG. 9: a) Butterfly hysteresis for the reference ferromagnet SrRuO₃ at 160K (i.e., just below $T_c = 165K$, its ordering temperature). Filled circles designate the virgin hysteresis branch, characterized by no maximum or other features. Note the response for increasing and decreasing H_{dc} are opposite to that of Ru-1222. b) NIS for SrRuO₃ at 160K. Note that this hysteresis corresponds, by all means, to the standard ferromagnetic one.

ing time used to obtain the data, and iii) the presence of two- rather than the expected one- maxima per field-increasing or field-decreasing branch. As Fig. 8a shows, the virgin branch exhibits a maximum at a characteristic dc magnetic field (H_{sf}). In simple ferromagnets, the virgin curve typically does not exhibit a maximum²⁰ because the remanence, and thus coercive field¹⁹, builds up only after the first field swing, as shown for SrRuO₃ (Fig. 9a). The quantitative size of the butterfly hysteresis loop depends on the observation time, which is another indication that the metastable magnetic states are involved. Qualitatively, though, over the range of sweep times we studied (one minute to one day), the inverted butterfly loops exhibit the same features. Also noteworthy is that the field H_{sf} is close to the minimum field needed to apply in order to obtain closed butterfly loops: if the range of sweeping field was narrower than $(-H_{sf}, +H_{sf})$ no closed loops would be observed whatever. Instead, the AC susceptibility signal would merely systematically diminish from cycle to cycle. Fig. 10a illustrates how H_{sf} and α_{off} , the logarithmic relaxation rate, change with temperature. The two parameters-logarithmic relaxation and inverted hysteretic behavior- exhibit virtually identical temperature dependence, indicating that the two phenomena have a common origin in Ru-1222. Another indi-

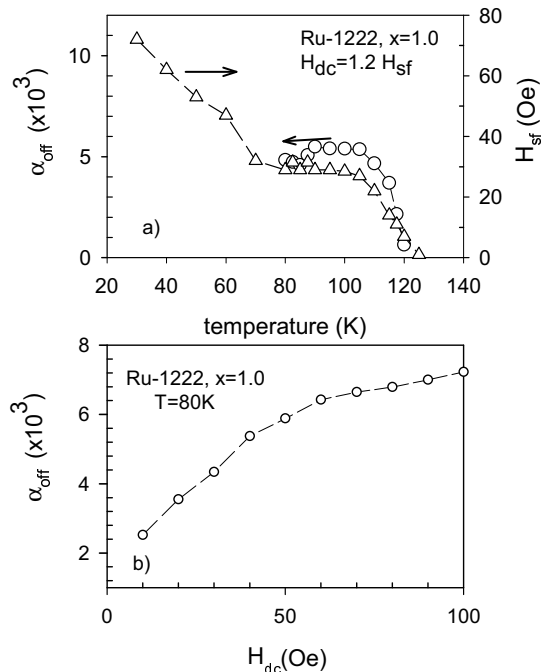


FIG. 10: a) Left axis: α_{off} , the relaxation rate constant defined in text, when H_{dc} is switched off, versus temperature. Right axis: The field attributed to spin flop, H_{sf} (Fig.8a), versus temperature. Note that both quantities are zero at temperatures above the susceptibility peak. b) α_{off} , at 80K, versus H_{dc} .

cation that the two phenomena are interrelated is shown in Fig. 10b. α_{off} changes rapidly in small dc magnetic fields, but saturates at $H_{dc} \geq H_{sf}$. Another commonality is the change of $\Delta\chi$ with H_{dc} (Fig. 6b, inset). $\Delta\chi$ becomes positive above H_{sf} and thereafter monotonically increases with increasing H_{dc} . Again, these qualitative changes in relaxation parameters are connected to the inverse hysteretic behavior.

IV. DISCUSSION

The first step to interpreting these results is to determine whether the results are intrinsic or extrinsic. The samples are polycrystalline, so extrinsic sources can include magnetic dynamics of single domain grains with intergranular magnetic interactions. A similar question has arisen^{21,22} in studies of polycrystalline $(La,Sr)_3Mn_2O_7$. For our samples, the microstructure (Fig. 2) indicates that the phenomena are intrinsic. The largest effects were measured on Ru-1222 ($x=1.0$) samples having barely detectable grain boundaries with large and densely packed crystalline grains. The effects are present in Ru-1222 ($x=0.5$) but absent in Ru-1222, although these samples have very similar microstructures with grain size of $1-2\mu m$ and pronounced grain boundaries. We conclude that the phenomena reported in Figs.3- 10 are predomi-

nantly intrinsic, due to magnetic interactions within the unit cell. The non-monotonic ZFC AC susceptibility for different dc magnetic fields (Fig. 4, 5) can be naturally interpreted as indicating the coexistence of antiferromagnetic (AFM) and ferromagnetic (FM) magnetic ordering in Ru-1222, with the magnetic order spontaneously occurring below T_M . As discussed further below, we argue that a small dc magnetic field partially cancels the AFM component, which increases the magnetization of the sample. This behavior leads to first an increase in AC susceptibility, with a decrease as H_{dc} increases further. A pronounced dependence of AC susceptibility on the balance between FM and AFM correlations has recently been reported²³ in $(La,Sr)_3Mn_2O_7$. Ref. 23 reports the onset and growth of AFM correlations, accompanied by a remarkable drop in the AC susceptibility, which is consistent with our interpretation. One noteworthy difference between this report and Ref. 23 is that in Ru-1222, the AFM contribution is tuned by the dc magnetic field, while in Ref. 23 the AFM correlations are controlled by varying the stoichiometry. By contrast to Ru-1222, Ru-1212 exhibits a monotonic decrease of the AC susceptibility with increasing dc magnetic field. In Ru-1212, Ref. 6 argues from neutron scattering data that there is a G-type AFM spontaneous magnetic order. We argue that applying a small (0- 100 Oe) dc magnetic field to Ru-1212 is not large enough to induce any FM order, while such small fields are sufficient in Ru-1222. The butterfly hysteresis data provides information about the nature of the AFM component of magnetic order. For Ru-1222, the hysteresis loop from AC susceptibility data is inverted. A theoretical model for such inverted hysteresis loops²⁴ indicate that inverted hysteresis loops can arise in exchange-coupled layered magnetic ‘sandwiches’ provided that the intralayer coupling is significantly larger than the interlayer coupling. The demagnetizing boundary effects, present in any real finite-size sample, was explicitly taken into account and shown to be crucial for the model predictions. Ref. 24 also calculated the conditions needed to assure that such inverted hysteresis loops not to violate the second law of thermodynamics. Previous experimental reports of inverted hysteresis loops^{25,26} have been limited to magnetic multilayers and nanoscale magnetic films. Ref. 25 argues that in their samples adjacent layers have magnetic moments with AFM coupling between adjacent layers. Ref. 25 also demonstrated that the inverted hysteresis loop behavior disappears in their samples if the AFM interlayer coupling is changed to a FM interlayer coupling. The present report, to our knowledge, is the first to show inverted hysteresis loops for bulk magnetic systems. We argue that the presence of such inverted hysteresis loops in Ru-1222 arises from RuO_2 layers with FM magnetic moments, combined with AFM coupling between the RuO_2 planes. A similar conclusion has recently been made for the layered manganite $(La,Sr)_3Mn_2O_7$ based on magneto- optical¹⁰ and neutron diffraction²⁷ data; in this compound the MnO_2 plays the role of the FM layers.

Observing inverted hysteresis loop behavior provides support for a magnetic multilayer scenario in Ru-1222. Arguing for AFM interlayer coupling, however, requires more specific experimental support. The most direct support would be evidence of a spin flop transition through which the net magnetization of adjacent, weakly AFM coupled, layers increases²⁸. Unfortunately, there are no single crystal samples of Ru-1222 available to obtain such direct evidence, e.g., by neutron diffraction. We argue, however, that our results support the presence of a spin flop transition at the characteristic field H_{sf} in favorably oriented grains of our polycrystalline Ru-1222 samples. It is important to note that the butterfly hysteresis loops we measured would close only for applied fields larger than H_{sf} , which is consistent with a spin flop transition and the onset of irreversible behavior. We attribute the maxima in the initial AC susceptibility data (Fig. 8a) to a spin flop transition. This assignment is quite similar to a recent report on AFM ordered chain-ladder compounds²⁹. In Ref. 29, the position of the susceptibility peak defines the spin flop field. This field is substantially higher in Ref. 29 than in this report due to the different nature of AFM interactions in the two systems. However, our experimental values of a spin flop field below 100 Oe is compatible with the field values measured in magnetic trilayer and multilayer systems, which are several orders of magnitude smaller than bulk AFM systems²⁸.

A. Model for magnetic coupling in Ru-1222

While our report does not include any determination of the magnetic structural order, the results are compatible with a simple model, shown schematically in Fig. 11. We start with the generally accepted model for the magnetic structure of the more thoroughly investigated, and simpler, Ru-1212. It is well established^{6,30} that the dominant magnetic order is a G-type antiferromagnetic structure in which the Ru moments are aligned antiparallel in all crystallographic directions. The details of the magnetic order, and the stability of a particular ground state⁸ can be interpreted only by explicitly including rotations and tilting of the RuO_6 octahedra and considering the orientation of the magnetic moments. A weak ferromagnetism originates from canting of the Ru moments³. The canting arises from the Dzyaloshinsky-Moriya³¹ antisymmetric superexchange interaction which, by symmetry, follows from the fact that the RuO_6 octahedra tilt away from the crystallographic c direction; there is still a controversy as to whether the tilting around the axis perpendicular to the c -axis is actually observed^{9,30,32}. In Ru-1212 samples containing magnetic (Gd) ions, the dipolar field of the in-plane ferromagnetic components induces an additional ferromagnetic component^{7,30}. Very recently, results of a structural investigation of the Ru-1222 compound ($x=1.0$) indicates that there are no important differences in rotation or tilting angles between the Ru-1212 and Ru-1222 ($x=1.0$) compounds⁹, in spite

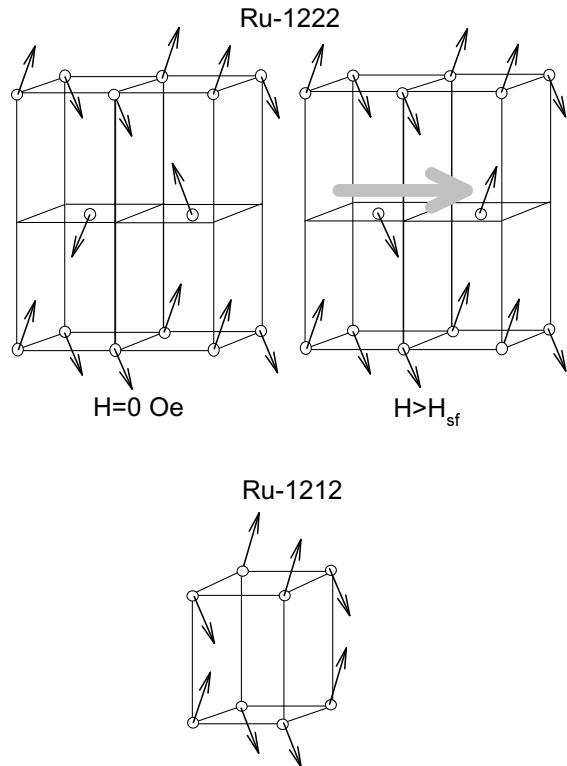


FIG. 11: Model for magnetic structure of Ru-1222. The region two unit cells wide is shown schematically. Circles designate the Ru-ions and arrows the associated magnetic moments. A widely accepted model³⁰ for magnetic structure of Ru-1212 is also shown for comparison. The global order is G-type antiferromagnetic in both systems. In Ru-1222, small ferromagnetic components-projection of the moments to the RuO_2 planes- are antiparallel in $H=0$. The in-plane components become mutually parallel - ferromagnetic- by application of small spin flop field H_{sf} . Thick grey arrow designates the field direction.

of Ru-1212 exhibiting dominant antiferromagnetic and Ru-1222 dominant ferromagnetic spontaneous magnetic order. We suggest that the magnetic ordering in both compounds is a variation of the G-type antiferromagnetism, while variation in dc magnetic properties, particularly in low fields, arises from small differences in the Ru-Ru interaction within their respective unit cells. The unit cells are different: in Ru-1222 there is a structural phase shift of half of the RuO_2 planes that leads to an approximate doubling of the unit cell. The phase shift arises from the presence of the fluorite- structure block $\text{Eu}_{2-x}\text{Ce}_x\text{O}_2$ replacing the rare earth ion in Ru-1212. Thus, in Ru-1222, nearest neighbor (Ru) ions are not vertically aligned, while they are in Ru-1212. This difference in structure naturally leads, in Ru-1222, to having the relative alignment of the in-plane components in adjacent RuO_2 planes antiparallel, which is energetically favored by a bare dipole-dipole interaction. Fig. 11 shows the magnetization tilting scheme we propose

for Ru-1222. Our experimental results fit quite naturally with such a picture: since the dipole interaction is very weak- the energy needed to reverse the in-plane Ru moment component is small- a small applied magnetic field can easily transform the spontaneous AF order, via a spin flop mechanism, into a ferromagnetic orientation. This is exactly what our measurements indicate. Our model is, apart from the unusual dipole-dipole interaction, the same as the models used to explain weakly AF coupled magnetic multilayers^{28,33}. We note that our model does not take into account the role of the (Ce), which is expected to have a non-zero magnetic moment. Our model is, however, of use in understanding the qualitative features of the Ru-1222 experimental data.

The most unusual feature of our model is the pronounced role of the dipole-dipole interaction; various magnetic exchange interactions (e.g., superexchange, double exchange) are more commonly employed to explain magnetic coupling. We argue that a dipole-dipole interaction makes sense because the nearest RuO₂ layers are far apart, with insulating and non-magnetic layers in between. Experimentally, the logarithmic time dependence of the magnetic relaxation (Fig. 6c) argues for the long-range dipole-dipole interaction; it is well known³⁴ that such a long-range interaction can account for a logarithmic relaxation behavior without further assumptions. We also considered the possibility that the logarithmic relaxation behavior might be due to domain-wall stabilization (disaccommodation) involving a broad range of activation energies, as has been recently applied to data in a perovskite manganite^{14,16}. However, one of us (IF) and colleagues have performed temperature-dependent x-ray diffraction studies of Ru-1222. The measurements indicate no structural change with temperature- such changes are necessary for disaccommodation³⁵. Thus both the weak AF coupling and the logarithmic susceptibility re-

laxation support our model.

V. CONCLUSION

In summary, we have presented data indicating that Ru-1222 exhibits qualitatively new magnetic behavior, including magnetic logarithmic relaxation, inverted hysteresis loops, and metastable magnetic states. None of these behaviors are observed in Ru-1212. Our results are interpreted within a model for the magnetic structure for Ru-1222 that, assuming a G-type AF global magnetic order known to describe Ru-1212, attributes the interlayer magnetic coupling to a dipole-dipole interaction. We interpret the hysteretic behavior as similar to that reported for magnetic multilayers, trilayers, and some manganites, due to spin flop transitions converting the spontaneous ($H = 0$) AF order between components into a ferromagnetic order.

Acknowledgments

We benefited from conversations with Robert Joynt. We also thank K. Zadro for the VSM measurements. Financial support was partially provided by the U.S.- Israel Binational Science Foundation, the U.S. D.O.E., the SCOPES program of the Swiss National Science Foundation, Fonds National Suisse de la Recherche Scientifique and EPFL.

Note added: After completion of this work and after the original version of the manuscript was submitted in short form³⁶, we became aware of two reports that are related to our report, including the work by Ohkoshi et.al.³⁷ on spin flip transitions in bulk materials, and by Y.Y. Xue et.al.³⁸ on RuSr₂(Gd,Ce)₂Cu₂O_{10-y} using magnetization.

* Electronic address: prester@ifs.hr

† Electronic address: onellion@landau.physics.wisc.edu

¹ *Superconductivity in Ternary Compounds*, edited by M.B. Maple and O. Fischer, Springer-Verlag, Berlin 1982.

² Y. Tokunaga, H. Kotegawa, K. Ishida, Y. Kitaoka, H. Takigiwa, and J. Akimitsu, Phys.Rev.Lett. 86, 5767 (2001).

³ I. Felner, U. Asaf, Y. Levi, and O. Millo, Phys.Rev.B 55,R3374 (1997).

⁴ C. Bernhard, J.L. Tallon, Ch. Niedermayer, Th. Blasius, A. Golnik, E. Brúcher, R.K. Kremer, D.R. Noakes, C.E. Stronach, and E.J. Ansaldo, Phys.Rev.B 59, 14099 (1999).

⁵ A. Feinstein, E. Winkler, A. Butera, and J. Tallon, Phys.Rev.B 60, R12597 (1999).

⁶ J.W. Lynn, B. Keimer, C. Ulrich, C. Bernhard, and J.L. Tallon, Phys.Rev.B 61, R14964 (2000).

⁷ G.V.M. Williams and S. Krámer, Phys.Rev.B 62, 4132 (2000).

⁸ K. Nakamura, K.T. Park, A.J. Freeman, and J. Jorgensen, Phys.Rev.B 63, 024507 (2001).

⁹ G.V. Williams et al. cond-mat/0108521.

¹⁰ U. Welp, A. Berger, D.J. Miller, V.K. Vlasko-Vlasov, K.E. Gray, and J.F. Mitchell, Phys.Rev.Lett. 20, 4180 (1999).

¹¹ H. Berger et al., unpublished.

¹² <http://www.cryobind.com>.

¹³ D. Ariosa et al., unpublished.

¹⁴ M. Muroi, R. Street, J.W. Cochrane, and G.J. Russell, Phys.Rev B 64, 024423(2001).

¹⁵ H. Kronmüller, Philos.Mag. B48, 127 (1983).

¹⁶ M. Muroi, R. Street, J.W. Cochrane, and G.J. Russell, Phys.Rev.B 62, R9268(2000).

¹⁷ R. Street and S.D. Brown, J.Appl.Phys. 76, 6386 (1994).

¹⁸ F.H. Salas and D. Weller, JMMM 128, 209 (1993), and references therein.

¹⁹ The equivalency of butterfly and magnetization hysteresis is simple consequence of the relationship: $M(H) = \int_0^H \chi(h)dh$ valid - up to an integration constant- in simple isotropic ferromagnets. However, in complex magnetic systems replacing χ (a tensor) by a scalar is not approved and the relationship does not hold.

- ²⁰ In principle, the observed maximum could be ascribed to a cross over between reversible and irreversible dynamics of ferromagnetic domains. However, the idea of reversibility, at least in its elementary form, is incompatible with logarithmic relaxations characterizing the whole 0-100 Oe range. Therefore, it seems that the latter interpretation cannot be applied in its original transparent form.
- ²¹ A. Gupta, G.Q. Gong, G. Xiao, P.R. Duncombe, P. Leceoeur, P. Trouilloud, Y.Y. Wang, V.P. Dravid, and J.Z. Sun, *Phys.Rev. B* 54, R15629 (1996).
- ²² H.Y. Hwang, S-W. Cheong, N.P. Ong, and B. Batlogg, *Phys.Rev.Lett* 77, 2041(1996).
- ²³ S.I. Patil, S.M. Bhagat, S.B. Ogale, Q.Q. Shu, and S.E. Lofland, *J.Appl.Phys.* 87, 5028 (2000).
- ²⁴ A. Aharoni, *J.Appl.Phys.* 76,6977 (1994).
- ²⁵ P. Pouloupoulos, R. Krishnan, and N.K. Flevaris, *JMMM* 163, 27 (1996), and references therein.
- ²⁶ M. Cougo dos Santos, J. Geshev, J.E. Schmidt, S.R. Teixeira, and L.G. Pereira, *Phys.Rev.B* 61, 1311 (2000).
- ²⁷ T.G. Perring, G. Aeppli, T. Kimura, Y. Tokura, and M.A. Adams, *Phys.Rev.B* 58, R14693 (1998).
- ²⁸ B. Dieny, J.P. Gavigan, and J.P. Rebouillat, *J.Phys.:Condens.Matter* 2,159(1990); B. Dieny and J.P. Gavigan, *ibid.* 187.
- ²⁹ M. Isobe, Y. Uchida, and E. Takayama-Muromachi, *Phys.Rev.B* 59, 8703 (1999).
- ³⁰ J.D. Jorgensen, O. Chmaissem, H. Shaked., S. Short, P.W. Klamut, B. Dabrowski, and J.L. Tallon, *PRB* 63, 05440 (2001).
- ³¹ T. Moriya, *Phys.Rev.*120, 91 (1960).
- ³² A.C. McLaughlin, W. Zhou, J.P. Attfield, A.N. Fitch, and J.L. Tallon, *Phys.Rev.B* 60, 7512 (2000).
- ³³ G.A. Prinz, *Science* 282, 1660 (1998), and references therein.
- ³⁴ D.K. Lottis, R.M. White, and E.D. Dahlberg, *Phys.Rev.Lett.*67, 362 (1991);
- ³⁵ I. Felner I, E.B. Sonin, T. Machi, N.I. Koshizuka, *Physica C*, 341-348, 715 (2000).
- ³⁶ I. Živković et al., *cond-mat/0107388*.
- ³⁷ S. Ohkoshi, T. Hozumi, and K. Hashimoto, *Phys.Rev.B* 64, 132404 (2001).
- ³⁸ Y.Y. Xue, D.H. Cao, B. Lorenz, and C.W. Chu, *cond-mat/0109500*.